

Evaluation of Lyapunov Function Candidates through Averaging Iterations

Carlos Argáez¹ ^a, Peter Giesl² ^b and Sigurdur Hafstein¹ ^c

¹Science Institute, University of Iceland, Dunhagi 3, 107 Reykjavík, Iceland

²Department of Mathematics, University of Sussex, Falmer, BN1 9QH, U.K.

Keywords: Complete Lyapunov Functions, Chain-recurrent Set, Numerical Methods, Dynamical Systems, Iterative Methods.

Abstract: A complete Lyapunov function determines the behaviour of a dynamical system. In particular, it splits the phase space into the chain-recurrent set, where solutions show (almost) repetitive behaviour, and the part exhibiting gradient-like flow where the dynamics are transient. Moreover, it reveals the stability of sets and basins of attraction through its sublevel sets. In this paper, we combine two previous methods to compute complete Lyapunov functions: we employ quadratic optimization with equality and inequality constraints to compute a complete Lyapunov function candidate and we evaluate its quality by using a method that improves approximations of complete Lyapunov function candidates through iterations.

1 INTRODUCTION

Consider a general autonomous ODE:

$$\dot{\mathbf{x}} = \mathbf{f}(\mathbf{x}), \text{ where } \mathbf{x} \in \mathbb{R}^n. \quad (1)$$

A complete Lyapunov function (CLF) candidate is a function $V: \mathbb{R}^n \rightarrow \mathbb{R}$ which is constant or decreasing along solutions of (1). If V is smooth, then this can be expressed by the fact that its orbital derivative, i.e. the derivative along solutions, is negative or zero. In formula, this reads $\nabla V(\mathbf{x}) \cdot \mathbf{f}(\mathbf{x}) \leq 0$.


A CLF candidate delivers information about the qualitative behaviour of (1). The larger the area of the phase space, where V is strictly decreasing, the more information can be obtained from the CLF candidate. The region in which the solution to (1) shows (almost) repetitive behaviour, i.e. the chain-recurrent set, is necessarily contained in the set where $\nabla V(\mathbf{x}) \cdot \mathbf{f}(\mathbf{x}) = 0$.


The first proof of the existence of a CLFs for dynamical systems was given by Conley (Conley, 1978). This proof holds for a compact metric space and it considers each corresponding attractor-repeller pair and constructs a function which is 1 on the repeller, 0 on the attractor and decreasing in between. Then


these functions are summed up over all attractor-repeller pairs. Later, Hurley generalized these ideas to more general spaces (Hurley, 1992; Hurley, 1998). These functions, however, are just continuous functions. In (Fathi and Pageault, 2019) and (Bernard and Suhr, 2018; Suhr and Hafstein, 2020) the existence of smooth CLFs for ODEs on compact and noncompact phase spaces was proved, respectively.

Computational approaches to construct CLFs have been proposed in (Kalies et al., 2005; Ban and Kalies, 2006; Goulet et al., 2015), where the phase space was subdivided into cells, defining a discrete-time system given by the multivalued time- T map between them. This multivalued map was then computed using the computer package GAIO (Dellnitz et al., 2001). Hence, an approximate complete Lyapunov function was constructed using graph algorithms (Ban and Kalies, 2006). This approach requires a high number of cells even for low dimensions. In (Björnsson et al., 2015), a CLF was constructed as a continuous piecewise affine (CPA) function on a fixed simplicial complex. However, it is assumed that information about the location of local attractors is available.

In this paper we consider two different methods, which have previously been proposed to compute CLF candidates. Both use collocation with radial basis functions (RBF) to parameterize a CLF candidate. In the first method quadratic programming (Giesl et al., 2018) is used to compute a norm-minimal so-

^a  <https://orcid.org/0000-0002-0455-8015>

^b  <https://orcid.org/0000-0003-1421-6980>

^c  <https://orcid.org/0000-0003-0073-2765>

lution with differential equality and inequality constraints. The second method solves a well-posed discretization of an ill-posed PDE (Argáez et al., 2017; Argáez et al., 2018a; Argáez et al., 2018b; Argáez et al., 2018c). By examining where the solution to the discretized problem delivers a poor approximation to the original PDE, information about the location of the chain-recurrent set is obtained. In subsequent iterations the right-hand side of the PDE is modified to include information from previous solutions and numerical evidence suggests that a good estimate on the chain-recurrent set is delivered after sufficiently many iterations.

In this paper we will investigate the local optimality of the norm-minimal solution to the quadratic minimization problem from (Giesl et al., 2018). In detail, we will use the norm-minimal solution as the initial value to the iterative method from (Argáez et al., 2018c) and see how much it improves. This gives us an indication of how optimal, in the sense of delivering a reasonable estimate on the chain-recurrent set, the norm-minimal solution to the quadratic optimization problem is.

The structure of the paper is as follows: In Section 2 we briefly describe meshfree collocation methods using RBF and then we give a short description of the quadratic optimization method and the iterative PDE method to compute CLF candidates. Then, in Section 3 we present our new algorithm to evaluate the norm-minimal solution to the quadratic optimization problem using the iterative PDE method. In Section 3.2 we numerically investigate three planar systems using our new method with two different support parameters for the radial basis functions and in Section 4 we draw conclusions from our results.

2 THE COMPUTATIONAL METHODS

We first give a short review of collocation methods using meshfree collocation of RBFs, before we describe the methods to compute CLF candidates using quadratic optimization and iteratively solving PDEs.

2.1 Meshfree Collocation

Meshfree collocation with RBFs can be used to solve generalized interpolation problems. A classical interpolation problem is, given finitely many points $\mathbf{x}_1, \dots, \mathbf{x}_N \in \mathbb{R}^n$ and corresponding values $r_1, \dots, r_N \in \mathbb{R}$, to find a function v satisfying $v(\mathbf{x}_j) = r_j$ for all $j = 1, \dots, N$.

Solving a PDE of the form $LV(\mathbf{x}) = r(\mathbf{x})$, where L denotes a differential operator, is a generalized interpolation problem as we look for a function v satisfying $Lv(\mathbf{x}_j) = r_j$ for all $j = 1, \dots, N$, where again finitely many points $\mathbf{x}_1, \dots, \mathbf{x}_N \in \mathbb{R}^n$ and values $r_1 = r(\mathbf{x}_1), \dots, r_N = r(\mathbf{x}_N) \in \mathbb{R}$ are given.

The approximating functions will belong to a Hilbert space H , which we assume to have a reproducing kernel $\Phi : \mathbb{R}^n \times \mathbb{R}^n \rightarrow \mathbb{R}$, given by a RBF ψ_0 through $\Phi(\mathbf{x}, \mathbf{y}) := \psi_0(\|\mathbf{x} - \mathbf{y}\|_2)$.

In general, we seek to reconstruct the target function $V \in H$ from the information $r_1, \dots, r_N \in \mathbb{R}$ generated by N linearly independent functionals $\lambda_j \in H^*$, i.e. $\lambda_j(V) = r_j$ holds for $j = 1, \dots, N$. The optimal (norm-minimal) reconstruction of the function V is the solution of the problem in H :

$$\min\{\|v\|_H : \lambda_j(v) = r_j, 1 \leq j \leq N\}. \quad (2)$$

It is well known (Wendland, 2005) that the optimal reconstruction can be represented as a linear combination of the Riesz representatives $v_j \in H$ of the functionals and that these are given by $v_j = \lambda_j^y \Phi(\cdot, \mathbf{y})$, i.e. the functional applied to one of the arguments of the reproducing kernel. Hence, the solution can be written as

$$v(\mathbf{x}) = \sum_{j=1}^N \beta_j \lambda_j^y \Phi(\mathbf{x}, \mathbf{y}), \quad (3)$$

where the coefficients β_j are determined by the interpolation conditions $\lambda_j(v) = r_j, 1 \leq j \leq N$.

Consider now the PDE $LV(\mathbf{x}) = r(\mathbf{x})$, where $r(\mathbf{x})$ is a given function and L denotes the linear operator of the orbital derivative $LV(\mathbf{x}) = V'(\mathbf{x}) = \nabla V(\mathbf{x}) \cdot \mathbf{f}(\mathbf{x})$. We choose N pairwise distinct points $\mathbf{x}_1, \dots, \mathbf{x}_N \in \mathbb{R}^n$ of the phase space, which are not equilibria, i.e. $\mathbf{f}(\mathbf{x}_j) \neq \mathbf{0}$ for all $j = 1, \dots, N$, and define functionals $\lambda_j(v) := (\delta_{\mathbf{x}_j} \circ L)^x v = v'(\mathbf{x}_j) = \nabla v(\mathbf{x}_j) \cdot \mathbf{f}(\mathbf{x}_j)$, where δ is Dirac's delta distribution. The information is given by the right-hand side $r_j = r(\mathbf{x}_j)$ for all $1 \leq j \leq N$. The approximation is then

$$v(\mathbf{x}) = \sum_{j=1}^N \beta_j (\delta_{\mathbf{x}_j} \circ L)^y \Phi(\mathbf{x}, \mathbf{y}), \quad (4)$$

where the coefficients $\beta_j \in \mathbb{R}$ can be calculated by solving the system $A\beta = \mathbf{r}$ of N linear equations. Here, A is the $N \times N$ matrix with entries

$$\begin{aligned} a_{ij} &= (\delta_{\mathbf{x}_i} \circ L)^x (\delta_{\mathbf{x}_j} \circ L)^y \Phi(\mathbf{x}, \mathbf{y}) \\ &= \langle \lambda_i^y \Phi(\cdot, \mathbf{y}), \lambda_j^x \Phi(\cdot, \mathbf{z}) \rangle_H. \end{aligned} \quad (5)$$

The matrix A is positive definite, since the $\lambda_i \in H^*$ are linearly independent.

If the PDE has a solution V , then the error $\|LV - V\|_{L_\infty}$ can be estimated in terms of the so-called

fill distance which measures how dense the points $\{\mathbf{x}_1, \dots, \mathbf{x}_N\}$ are. In this case, v is the approximation to V . For the construction of a classical Lyapunov function for an equilibrium such error estimates were derived in (Giesl, 2007; Giesl and Wendland, 2007), see also (Narcowich et al., 2005; Wendland, 2005).

Meshfree collocation is well suited for solving PDEs because scattered points can be added, no triangulation of the phase space is necessary, the approximating function is smooth and the method works in any dimension.

In this paper, we use Wendland functions (Wendland, 1995; Wendland, 1998) as radial basis functions through $\psi_0(r) := \psi_{l,k}(cr)$, where $c > 0$, $k \in \mathbb{N}$ is a smoothness parameter and $l = \lfloor \frac{n}{2} \rfloor + k + 1$. Wendland functions are positive definite functions with compact support, which are polynomials on their support; the corresponding reproducing kernel Hilbert space is norm-equivalent to the Sobolev space $W_2^{k+(n+1)/2}(\mathbb{R}^n)$. They are defined by recursion: for $l \in \mathbb{N}$, $k \in \mathbb{N}_0$ we define

$$\psi_{l,0}(r) = (1-r)_+^l \tag{6}$$

$$\psi_{l,k+1}(r) = \int_r^1 t \psi_{l,k}(t) dt$$

for $r \in \mathbb{R}_0^+$, where $x_+ = x$ for $x \geq 0$ and $x_+ = 0$ for $x < 0$.

The parameter $c > 0$ controls the size of the support of the RBF, i.e. the support is a sphere of radius c^{-1} in the Euclidian norm centred at the origin.

We define recursively $\psi_i(r) = \frac{1}{r} \frac{d\psi_{i-1}}{dr}(r)$ for $i = 1, 2$ and $r > 0$. Note that $\lim_{r \rightarrow 0} \psi_i(r)$ exists if the smoothness parameter k of the Wendland function is sufficiently large. The explicit formulas for v and its orbital derivative are then, see (4)

$$v(\mathbf{x}) = \sum_{j=1}^N \beta_j \langle \mathbf{x}_j - \mathbf{x}, \mathbf{f}(\mathbf{x}_j) \rangle \psi_1(\|\mathbf{x} - \mathbf{x}_j\|_2),$$

$$v'(\mathbf{x}) = \sum_{j=1}^N \beta_j \left[-\psi_1(\|\mathbf{x} - \mathbf{x}_j\|_2) \langle \mathbf{f}(\mathbf{x}), \mathbf{f}(\mathbf{x}_j) \rangle \right. \tag{7}$$

$$\left. + \psi_2(\|\mathbf{x} - \mathbf{x}_j\|_2) \langle \mathbf{x} - \mathbf{x}_j, \mathbf{f}(\mathbf{x}) \rangle \cdot \langle \mathbf{x}_j - \mathbf{x}, \mathbf{f}(\mathbf{x}_j) \rangle \right]$$

where $\langle \cdot, \cdot \rangle$ denotes the standard scalar product in \mathbb{R}^n . The matrix elements of A are

$$a_{ij} = \psi_2(\|\mathbf{x}_i - \mathbf{x}_j\|_2) \langle \mathbf{x}_i - \mathbf{x}_j, \mathbf{f}(\mathbf{x}_i) \rangle \langle \mathbf{x}_j - \mathbf{x}_i, \mathbf{f}(\mathbf{x}_j) \rangle - \psi_1(\|\mathbf{x}_i - \mathbf{x}_j\|_2) \langle \mathbf{f}(\mathbf{x}_i), \mathbf{f}(\mathbf{x}_j) \rangle \tag{8}$$

More detailed explanations on this construction are given in (Giesl, 2007, Chapter 3).

2.2 CLFs via Quadratic Programming

In (Giesl et al., 2018) a novel method to compute CLF candidates via quadratic programming was proposed.

This approach reflects the definition of a CLF candidate, using differential inequalities rather than equalities. In particular, a CLF candidate V needs to satisfy $V'(\mathbf{x}) \leq 0$ because V is non-increasing. This makes the following requirement natural:

$$V'(\mathbf{x}) \begin{cases} = -1 & \text{for } \mathbf{x} \in X^- \\ \leq 0 & \text{for } \mathbf{x} \in X^0 \end{cases} \tag{9}$$

where $X = X^- \cup X^0$ is the collocation grid,

$$X^- = \{\mathbf{x}_{-M+1}, \dots, \mathbf{x}_0\}, \tag{10}$$

$$X^0 = \{\mathbf{x}_1, \dots, \mathbf{x}_N\} \tag{11}$$

and X^- must only include points in the subset of the phase space where the flow is gradient-like.

In correspondence with general interpolation problems delivering the norm-minimal solution as in (2) we seek to minimize $\|V\|_H$ with the constraints given by (9).

Thus with the functionals $\lambda_j = \delta_{\mathbf{x}_j} \circ L$ for $j = -M+1, \dots, N$ we consider the optimization problem:

$$\begin{cases} \text{minimize} & \|v\|_H \\ \text{subject to} & \lambda_j(v) = -1, j = -M+1, \dots, 0 \\ & \lambda_i(v) \leq 0, i = 1, \dots, N \end{cases} \tag{12}$$

where H is a reproducing kernel Hilbert space with kernel Φ , inner product $\langle \cdot, \cdot \rangle_H$ and norm $\|\cdot\|_H := \sqrt{\langle \cdot, \cdot \rangle_H}$. If all points $\mathbf{x}_{-M+1}, \dots, \mathbf{x}_N$ are pairwise distinct and no equilibrium points of (1), then the $\lambda_i \in H^*$ are linearly independent and it was shown in (Giesl et al., 2018) that (12) possesses a unique solution s^* .

A function of the form

$$v(\mathbf{x}) = \sum_{j=1}^N \beta_j \lambda_j^y \Phi(\mathbf{x}, \mathbf{y})$$

has the following norm in H

$$\begin{aligned} \|v\|_H^2 &= \left\langle \sum_{i=1}^N \beta_i \lambda_i^y \Phi(\cdot, \mathbf{y}), \sum_{j=1}^N \beta_j \lambda_j^z \Phi(\cdot, \mathbf{z}) \right\rangle_H \\ &= \sum_{i,j=1}^N \beta_i \beta_j \langle \lambda_i^y \Phi(\cdot, \mathbf{y}), \lambda_j^z \Phi(\cdot, \mathbf{z}) \rangle_H \\ &= \sum_{i,j=1}^N \beta_i \beta_j a_{ij} \\ &= \beta^T A \beta. \end{aligned}$$

This can be used, cf. (Giesl et al., 2018), to show that the solution s^* of (12) is of the form

$$s^*(\mathbf{x}) = \sum_{j=1}^N \beta_j \lambda_j^y \Phi(\mathbf{x}, \mathbf{y}), \tag{13}$$

where the coefficients β_j satisfy

$$\begin{cases} \text{minimize} & \beta^T A \beta \\ \text{subject to} & B_- \beta = -\mathbf{1} \in \mathbb{R}^M \\ \text{and} & B_0 \beta \leq \mathbf{0} \in \mathbb{R}^N \end{cases} \quad (14)$$

Here, the inequality is to be read componentwise, the matrix elements a_{ij} are defined by (5) and the matrices by

$$\begin{aligned} A &= (a_{ij})_{i,j=-M+1,\dots,N} \in \mathbb{R}^{(M+N) \times (M+N)} \\ &= \begin{pmatrix} A_{11} & A_{12} \\ A_{21} & A_{22} \end{pmatrix} \\ B_- &= (a_{ij})_{i=-M+1,\dots,0,j=-M+1,\dots,N} \in \mathbb{R}^{M \times (M+N)} \\ &= \begin{pmatrix} A_{11} & A_{12} \end{pmatrix} \\ B_0 &= (a_{ij})_{i=1,\dots,N,j=-M+1,\dots,N} \in \mathbb{R}^{N \times (M+N)} \\ &= \begin{pmatrix} A_{21} & A_{22} \end{pmatrix}. \end{aligned}$$

Since the λ_i are linearly independent, the matrices A , A_{11} and A_{22} are symmetric and positive definite, i.e. in particular $A_{11}^T = A_{11}$ and $A_{12}^T = A_{21}$, since they are part of the symmetric matrix A .

Note that the optimization problem (14) is a classical quadratic optimization problem that can be efficiently solved.

In our applications we choose $X^- = \{\mathbf{x}_0\}$ to be one point ($M = 1$) and N further, pairwise distinct points in the set X^0 . Recall that all points in $X = X^- \cup X^0$ are assumed not to be equilibria.

2.3 Iterative Averaging Method

In (Argáez et al., 2017; Argáez et al., 2018a; Argáez et al., 2018b; Argáez et al., 2018c) the following approach was followed for computing CLF candidates for the system (1): First, the ill-posed PDE

$$V'(\mathbf{x}) = \nabla V(\mathbf{x}) \cdot \mathbf{f}(\mathbf{x}) = -1$$

was discretized using meshfree collocation. The PDE is ill-posed because on the chain-recurrent set, including equilibria and periodic orbits, a function fulfilling the PDE cannot exist. The approximation with meshfree collocation fixes finitely many collocation points $X \subset \mathbb{R}^n$, and computes the norm-minimal function such that $V'(\mathbf{x}) = \nabla V(\mathbf{x}) \cdot \mathbf{f}(\mathbf{x})$ is fulfilled at these points. Thus, it delivers a solution, even if the underlying PDE does not have a solution. By evaluating the solution v_1 to the discretized problem and analysing where it does not fulfill the original PDE, one obtains an estimate of the location of the chain-recurrent set.

As collocation points $X = \{\mathbf{x}_1, \dots, \mathbf{x}_N\} \subset \mathbb{R}^n$ we use a hexagonal grid with fineness parameter $\alpha_{\text{Hexa-basis}} \in \mathbb{R}^+$, from which all equilibrium points have been removed. This grid is described in detail in

(Giesl, 2007; Argáez et al., 2017) and has been shown to deliver the optimal ratio of fill-distance and separation distance (Iske, 1998), which is desirable when using RBF.

By iterating this method by using the average $p(\mathbf{x})$ of v'_1 around \mathbf{x} as a new right-hand side and solving the PDE

$$V'(\mathbf{x}) = p(\mathbf{x}),$$

again using meshfree collocation, we obtain a new solution v_2 which is a better CLF candidate than v_1 . In practice one averages v'_1 across an evaluation grid $Y_{\mathbf{x}_j}$ around each collocation point $\mathbf{x}_j \in X$ and considers the discrete generalized minimization problem

$$V'(\mathbf{x}_i) = p(\mathbf{x}_i). \quad (15)$$

The evaluation grid is defined in (16), see (Argáez et al., 2018c), where more details are available.

$$Y_{\mathbf{x}_j} = \left\{ \mathbf{x}_j \pm \frac{r \cdot k \cdot \alpha_{\text{Hexa-basis}} \cdot \hat{\mathbf{f}}(\mathbf{x}_j)}{m} : k \in \{1, \dots, m\} \right\}, \quad (16)$$

where $r \in (0, 1)$ and m represent the amount of evaluation points per collocation point.

This method is studied in detail in (Argáez et al., 2017; Argáez et al., 2018a; Argáez et al., 2018b; Argáez et al., 2018c) and we do not go into details here. Just a few comments on the implementation:

First, it is advantageous to consider replacing the system (1) by the ODE (17)

$$\dot{\mathbf{x}} = \hat{\mathbf{f}}(\mathbf{x}), \quad \text{where} \quad \hat{\mathbf{f}}(\mathbf{x}) = \frac{\mathbf{f}(\mathbf{x})}{\sqrt{\delta^2 + \|\mathbf{f}(\mathbf{x})\|^2}} \quad (17)$$

with a small parameter $\delta > 0$. This new ODE has the same solutions as (1), but a more uniform speed. This was shown to reduce the over-estimation of the chain-recurrent set, i.e. the ‘‘noise’’ in the approximation. Further, as we show in Table 1, the condition numbers of the matrix A in the generalized minimization problem are several orders of magnitude lower than when using (1).

Second, there are several choices of evaluation grids possible. We use an evaluation grid aligned along the flow at each collocation point for the iterations (16), see (Argáez et al., 2018a).

Further, as we require $\nabla V(\mathbf{x}) \cdot \mathbf{f}(\mathbf{x}) \leq 0$ we replace $p(\mathbf{x}_j)$ by zero if the average of v'_1 around \mathbf{x}_j is positive.

Third, to avoid the solutions v_i to converge to the zero function with growing i , we normalize the right-hand side (15) over the iterations, i.e. $\sum_{i=1}^N p(\mathbf{x}_i) = \text{const.}$

3 EVALUATION METHOD

We first use the quadratic optimization method from (Giesl et al., 2018) as described in Section 2.2 to compute a CLF candidate v_1 . Then we apply the averaging iterations, starting with this v_1 , as described in Section 2.3.

3.1 General Algorithm

Our general algorithm to compute CLFs can be summarized as follows:

1. Create the set of collocation points $X^- = \{\mathbf{x}_{-M+1}, \dots, \mathbf{x}_0\}$, $X^0 = \{\mathbf{x}_1, \dots, \mathbf{x}_N\}$, and set $X := X_0 \cup X^-$. Solve the quadratic optimization problem (14), obtaining v_i with $i = 1$.
2. To determine the right-hand side of $V'(\mathbf{x}_j) = p(\mathbf{x}_j)$ for the next iteration define

$$\tilde{r}_j = \left(\frac{1}{|Y_{\mathbf{x}_j}|} \sum_{\mathbf{y} \in Y_{\mathbf{x}_j}} v'_i(\mathbf{y}) \right)_{-}$$

where $x_- = x$ if $x < 0$ and $x_- = 0$ otherwise. Here $Y_{\mathbf{x}_j}$ is the evaluation grid corresponding to the collocation point \mathbf{x}_j and $|Y_{\mathbf{x}_j}|$ is its cardinality. Set $p(\mathbf{x}_j) = C\tilde{r}_j$, where $C = 1$ if $i = 1$ and otherwise $C > 0$ is a normalization constant such that $\sum_{j=-M+1}^N p(\mathbf{x}_j)$ is equal to the same sum from the last iteration.

3. Solve the generalized interpolation problem

$$V'(\mathbf{x}_j) = p(\mathbf{x}_j),$$

as described in Section 2.1 to obtain a solution v_{i+1} .

4. Set $i \rightarrow i + 1$ and repeat steps 2. and 3. until some predefined criterion is reached.

The convergence of this algorithm is considered to have been reached when a given number of iterations have been performed or when a sufficiently good approximation to the CLF is achieved. To obtain an estimate of the location of the chain-recurrent set from a solution v_i we evaluate it on a fine Cartesian grid. The set

$$\{\mathbf{x} : v'_i(\mathbf{x}) \geq -\gamma\},$$

where $\gamma \leq 0$ is some predefined parameter, is the approximation obtained from v_i .

It is known from (Argáez et al., 2017; Argáez et al., 2018a; Argáez et al., 2018b; Argáez et al., 2018c) that if we run the algorithm above with v_1 as a solution to the ill-posed PDE $V'(\mathbf{x}) = -1$, and not the solution to the quadratic optimization problem (14), this will result in a sequence of solutions v_i that give

successively better approximations of the location of the chain-recurrent set. The question we investigate in the next section is the following: if we start with v_1 as the solution to the quadratic optimization problem (14) from (Giesl et al., 2018), then does the approximation of the location of the chain-recurrent set improve, or is the solution v_1 optimal in the sense, that it cannot be improved by using averaging iterations.

3.2 Results

We consider three different planar systems from the literature and in all the examples we use a hexagonal grid with fineness parameter $\alpha_{\text{Hexa-basis}} \in \mathbb{R}^+$ as collocation grid $X = X_0$, from which all equilibrium points have been removed. In all the cases X^- consists of only one point \mathbf{x}_0 . Furthermore, we use $\Psi_{6,4}$ as Wendland function and two different support parameters, $c = 1$ and $c = 0.1$. Further, for determining the approximation to the chain-recurrent set we used a Cartesian grid $h\mathbb{Z}^2$ with $h = 0.03$ in all computations and we set the parameter $\gamma = 0$. Finally, we compared the chain-recurrent set obtained from the solution v_1 to the quadratic optimization problem (14) from (Giesl et al., 2018) (iteration 1) with v_{10} , i.e. the CLF candidate obtained from the algorithm in Section 3.1 after 10 iterations.

For each system we plot the CLF candidates v_1 and v_{10} , their orbital derivatives, and the approximation of the chain-recurrent set obtained from the CLF candidate.

3.2.1 Two Orbits

We consider system (1) with right-hand side

$$\mathbf{f}(x, y) = \begin{pmatrix} -x(x^2 + y^2 - 1/4)(x^2 + y^2 - 1) - y \\ -y(x^2 + y^2 - 1/4)(x^2 + y^2 - 1) + x \end{pmatrix}, \tag{18}$$

which has an asymptotically stable equilibrium at the origin, an asymptotically stable periodic orbit with radius 1, and a repelling periodic orbit with radius 1/2.

The collocation points were set in $(-1.5, 1.5) \times (-1.5, 1.5) \subset \mathbb{R}^2$ and we used $\alpha_{\text{Hexa-basis}} = 0.018$, which gives 32,064 collocation points. An extra point, $\mathbf{x}_0 = (0.1, 0)$ is added to fulfill the condition $v'(\mathbf{x}_0) = -1$ during the quadratic optimization.

Figure 1 shows the plots for v_1 and figure 2 shows the plots for v_{10} . Both figures used $c = 1$ for system (18). Likewise, figure 3 shows the plots for v_1 and figure 4 shows the plots for v_{10} . Both figures used $c = 0.1$ for system (18).

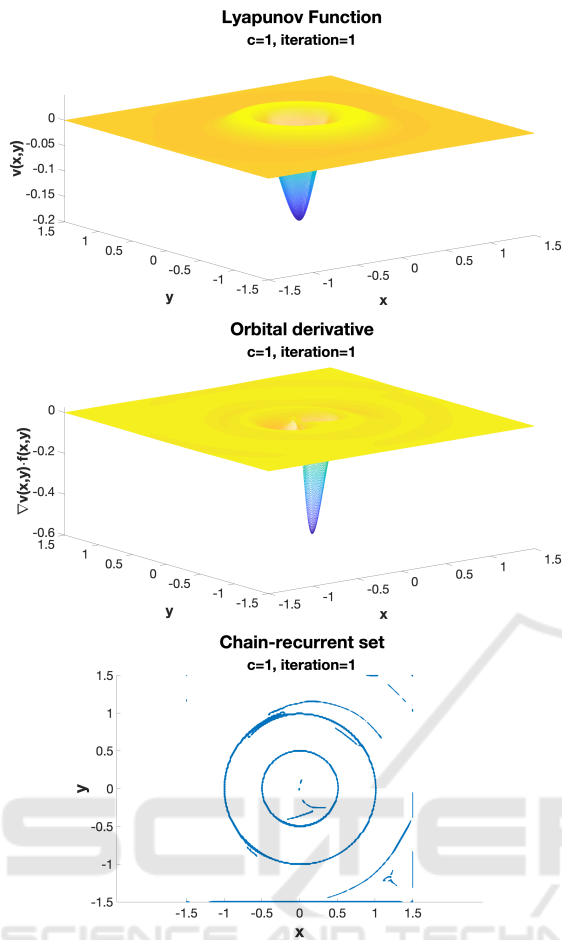


Figure 1: Above: Complete Lyapunov function. Middle: Orbital derivative. Bottom: Chain-recurrent set. System (18). First iteration, i.e., quadratic optimization. The normalized method was used with $c = 1$ and $\delta^2 = 10^{-8}$.

3.2.2 Homoclinic Orbit

We consider system (1) with right-hand side $\mathbf{f}(x,y) =$

$$\begin{pmatrix} x(1-x^2-y^2) - y((x-1)^2 + (x^2+y^2-1)^2) \\ y(1-x^2-y^2) + x((x-1)^2 + (x^2+y^2-1)^2) \end{pmatrix}. \quad (19)$$

This system has an unstable focus at the origin and an asymptotically stable homoclinic orbit at a circle centred at the origin and with radius 1.

The collocation points were set in $(-1.5, 1.5) \times (-1.5, 1.5) \subset \mathbb{R}^2$ with $\alpha_{\text{Hexa-basis}} = 0.018$, which gives 32,064 collocation points. An extra point, $\mathbf{x}_0 = (0.1846, 0)$ is added to fulfill the condition $v'(\mathbf{x}_0) = -1$ during the quadratic optimization.

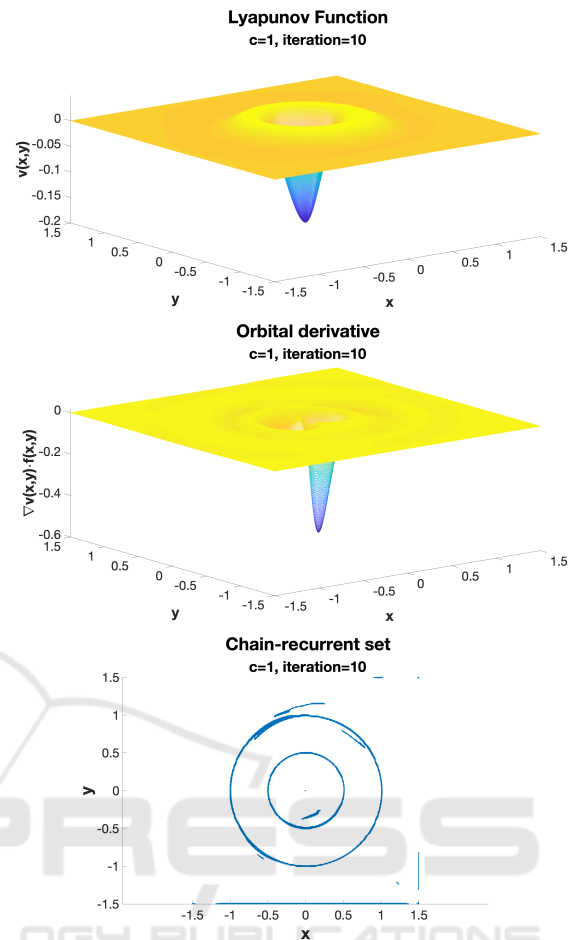


Figure 2: Above: Complete Lyapunov function. Middle: Orbital derivative. Bottom: Chain-recurrent set. System (18). Tenth iteration, i.e., iterative method solving the PDE to the values of the average values of the orbital derivatives around the corresponding collocation points. The normalized method was used with $c = 1$ and $\delta^2 = 10^{-8}$.

3.2.3 Van der Pol Oscillator System

We consider system (1) with right-hand side

$$\mathbf{f}(x,y) = \begin{pmatrix} y \\ (1-x^2)y - x \end{pmatrix}. \quad (20)$$

System (20) is the two-dimensional form of the Van der Pol oscillator. This describes the behaviour of a non-conservative oscillator reacting to a non-linear damping. The origin is an unstable focus, and the system has an asymptotically stable periodic orbit.

The collocation points were set in $(-4, 4) \times (-4, 4) \subset \mathbb{R}^2$ with $\alpha_{\text{Hexa-basis}} = 0.05$, which gives 29,440 collocation points. An extra point, $\mathbf{x}_0 = (0.1, 0)$ is added to fulfill the condition $V'(\mathbf{x}_0) = -1$ during the quadratic optimization.

Figure 5 shows the plots for v_1 and figure 6 shows the plots for v_{10} . Both figures used $c = 1$ for system

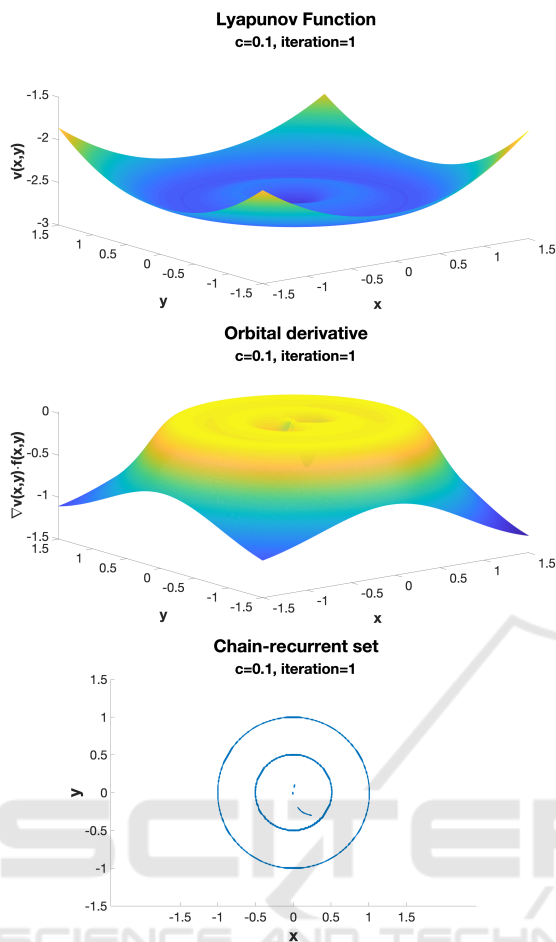


Figure 3: Above: Complete Lyapunov function. Middle: Orbital derivative. Bottom: Chain-recurrent set. System (18). First iteration, i.e., quadratic optimization. The normalized method was used with $c = 0.1$ and $\delta^2 = 10^{-8}$.

(19). Likewise, figure 7 shows the plots for v_1 and figure 8 shows the plots for v_{10} . Both figures used $c = 0.1$ for system (19).

Figure 9 shows the plots for v_1 and figure 10 shows the plots for v_{10} . Both figures used $c = 1$ for system (20). Likewise, figure 11 shows the plots for v_1 and figure 12 shows the plots for v_{10} . Both figures used $c = 0.1$ for system (20).

3.3 Discussion of the Results

Let us discuss the results from our examples (18), (19) and (20). Systems (19) and (20) do not show any improvement in the localization of the chain-recurrent set when using iterations as seen in figures 5,6,7,8,9, 10, 11 and 12. System (18) shows slight improvements, but only for $c = 1$. This clearly indicates that the solution v_1 to the quadratic optimization problem (14) from (Giesel et al., 2018) cannot be improved

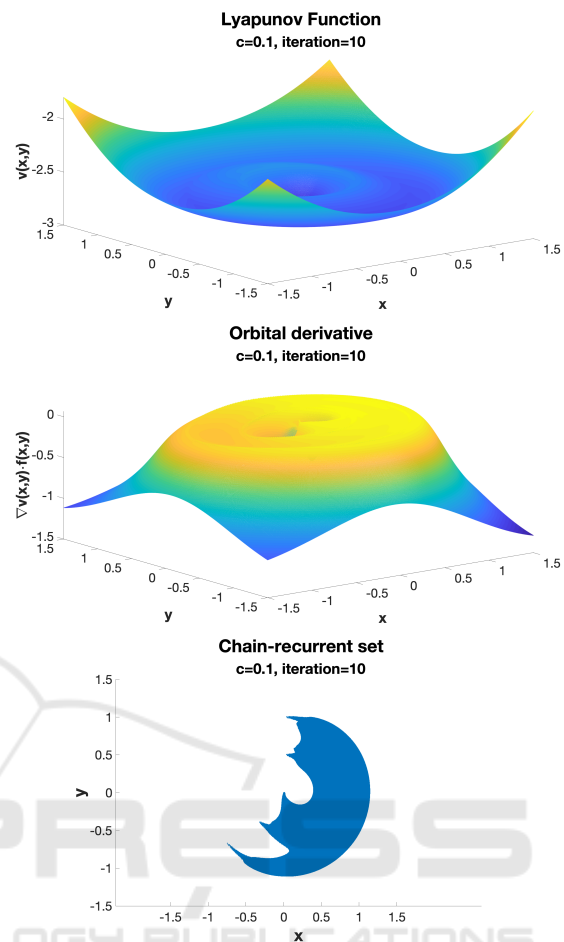


Figure 4: Above: Complete Lyapunov function. Middle: Orbital derivative. Bottom: Chain-recurrent set. System (18). Tenth iteration, i.e., iterative method solving the PDE to the values of the average values of the orbital derivatives around the corresponding collocation points. The normalized method was used with $c = 0.1$ and $\delta^2 = 10^{-8}$.

by averaging iterations. We conclude that the norm-minimization of the quadratic optimization problem delivers a locally optimal solution, in the sense, that averaging iterations do not improve the estimate of the chain-recurrent set. Indeed, the estimates become worse in most cases and, indeed, the approximation form v_1 is quite good.

However, as solving the quadratic optimization problem is much more computationally demanding than solving a system of linear equations and iterating, one might try to obtain a solution v_1 using only a few collocation points and then iterate on a denser grid. We will investigate this in the future.

Even if in this paper we have presented all our results with the normalized method, it is very informative to have a look at the condition numbers of the matrices involved in the examples, i.e. the matrix A

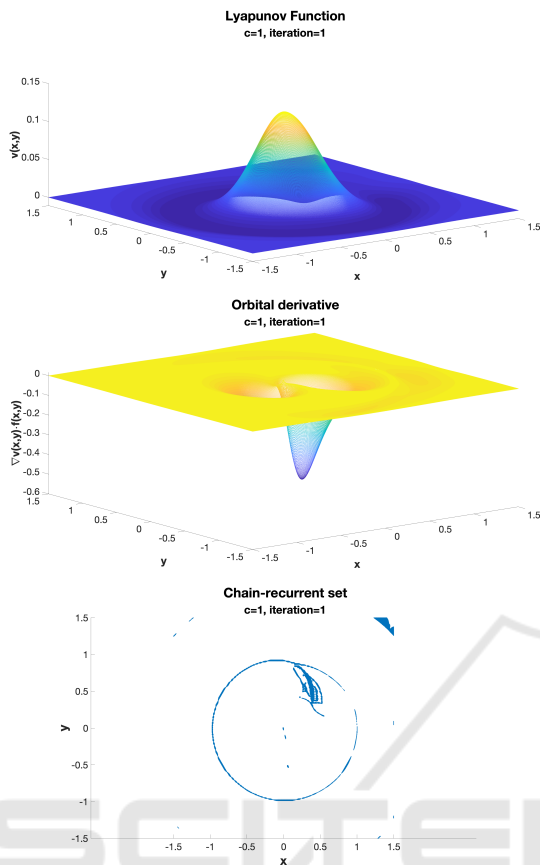


Figure 5: Above: Complete Lyapunov function. Middle: Orbital derivative. Bottom: Chain-recurrent set. System (19). First iteration, i.e., quadratic optimization. The normalized method was used with $c = 1$ and $\delta^2 = 10^{-8}$.

from the collocation with and without the normalized method.

Table 1: Condition number for the collocation matrices computed for all systems under different values of c . Using the system ODE directly on the left and normalized using (17) on the right.

	Condition number			
	Not normalized		Normalized as (17)	
	$c=1$	$c=0.1$	$c=1$	$c=0.1$
ODE (18)	10^{13}	10^{17}	10^8	10^{12}
ODE (19)	10^{15}	10^{19}	10^8	10^{12}
ODE (20)	10^{11}	10^{15}	10^6	10^{11}

As it can be seen collocation matrices computed with a Wendland function with support parameter $c = 0.1$ have much higher condition numbers, but this is to be expected as there is more overlap of supports, the matrix is less sparse, and the computed CLF candidate is in general of much higher quality. The more interesting observation is that using the normalization (17) of the right-hand side of the ODE to obtain a system

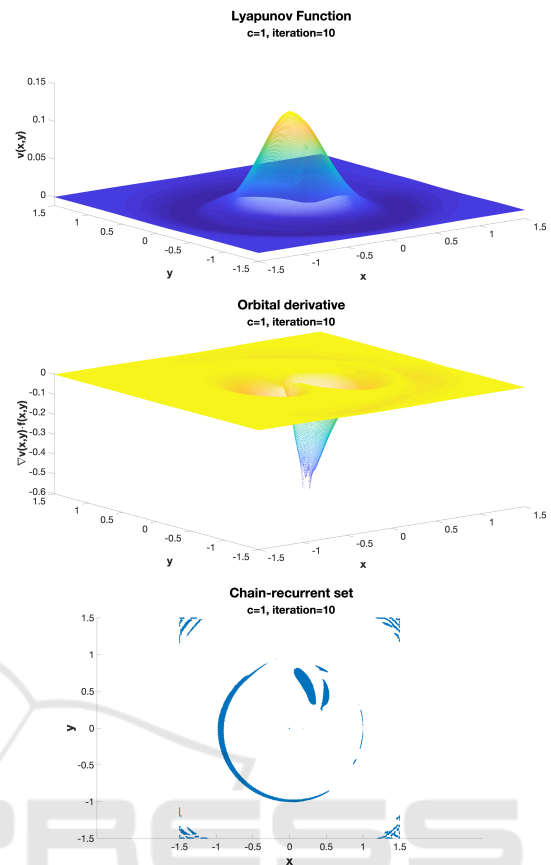


Figure 6: Above: Complete Lyapunov function. Middle: Orbital derivative. Bottom: Chain-recurrent set. System (19). Tenth iteration, i.e., iterative method solving the PDE to the values of the average values of the orbital derivatives around the corresponding collocation points. The normalized method was used with $c = 1$ and $\delta^2 = 10^{-8}$.

with a more uniform speed of traversing of trajectories delivers matrices with condition numbers that are several orders of magnitude lower.

4 CONCLUSIONS

We investigated whether a complete Lyapunov function candidate computed by quadratic optimization problem as in (Giesl et al., 2018) could be improved by applying averaging iterations from (Argáez et al., 2017; Argáez et al., 2018a; Argáez et al., 2018b; Argáez et al., 2018c), which have been shown to deliver successively better approximations when starting with an approximation to the ill-posed problem $V'(\mathbf{x}) = -1$. The result is that the complete Lyapunov function candidate obtained by quadratic optimization is locally optimal in the sense, that it cannot be improved by these iterations.

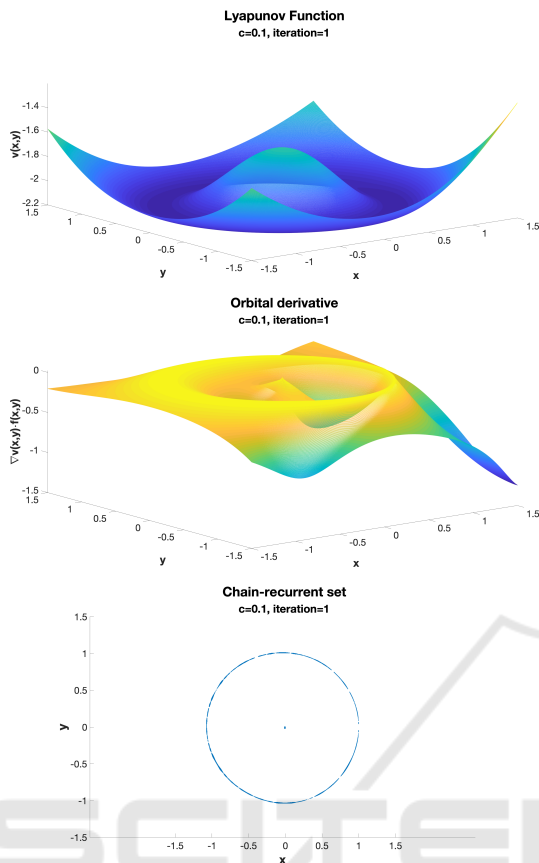


Figure 7: Above: Complete Lyapunov function. Middle: Orbital derivative. Bottom: Chain-recurrent set. System (19). First iteration, i.e., quadratic optimization. The normalized method was used with $c = 0.1$ and $\delta^2 = 10^{-8}$.

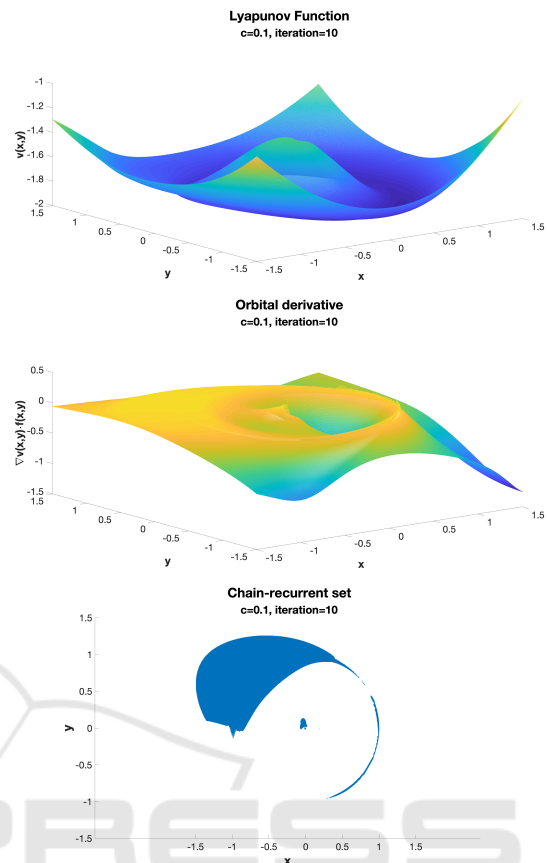


Figure 8: Above: Complete Lyapunov function. Middle: Orbital derivative. Bottom: Chain-recurrent set. System (19). Tenth iteration, i.e., iterative method solving the PDE to the values of the average values of the orbital derivatives around the corresponding collocation points. The normalized method was used with $c = 0.1$ and $\delta^2 = 10^{-8}$.

ACKNOWLEDGEMENTS

The research in this paper is supported by the Icelandic Research Fund (Rannís) grant number 163074-052, Complete Lyapunov functions: Efficient numerical computation.

REFERENCES

Argáez, C., Giesl, P., and Hafstein, S. (2017). Analysing dynamical systems towards computing complete Lyapunov functions. In *Proceedings of the 7th International Conference on Simulation and Modeling Methodologies, Technologies and Applications, Madrid, Spain*, pages 323–330.

Argáez, C., Giesl, P., and Hafstein, S. (2018a). Computation of complete Lyapunov functions for three-dimensional systems. In *Proceedings of the 57th IEEE Conference on Decision and Control (CDC)*, pages 4059–4064, Miami Beach, FL, USA.

Argáez, C., Giesl, P., and Hafstein, S. (2018b). Computational approach for complete Lyapunov functions. In *Awrejcewicz J. (eds) Dynamical Systems in Theoretical Perspective. DSTA 2017.*, volume 248. Springer Proceedings in Mathematics and Statistics. Springer, Cham.

Argáez, C., Giesl, P., and Hafstein, S. (2018c). Iterative construction of complete Lyapunov functions. In *Proceedings of 8th International Conference on Simulation and Modeling Methodologies, Technologies and Applications - Volume 1: SIMULTECH.*, pages 211–222. INSTICC, SciTePress.

Ban, H. and Kalies, W. (2006). A computational approach to Conley’s decomposition theorem. *J. Comput. Nonlinear Dynam.*, 1(4):312–319.

Bernard, P. and Suhr, S. (2018). Lyapunov functions of closed cone fields: from Conley theory to time functions. *Commun. Math. Phys.*, 359:467–498.

Björnsson, J., Giesl, P., Hafstein, S., Kellett, C., and Li, H. (2015). Computation of Lyapunov functions for systems with multiple attractors. *Discrete Contin. Dyn. Syst. Ser. A*, 35(9):4019–4039.

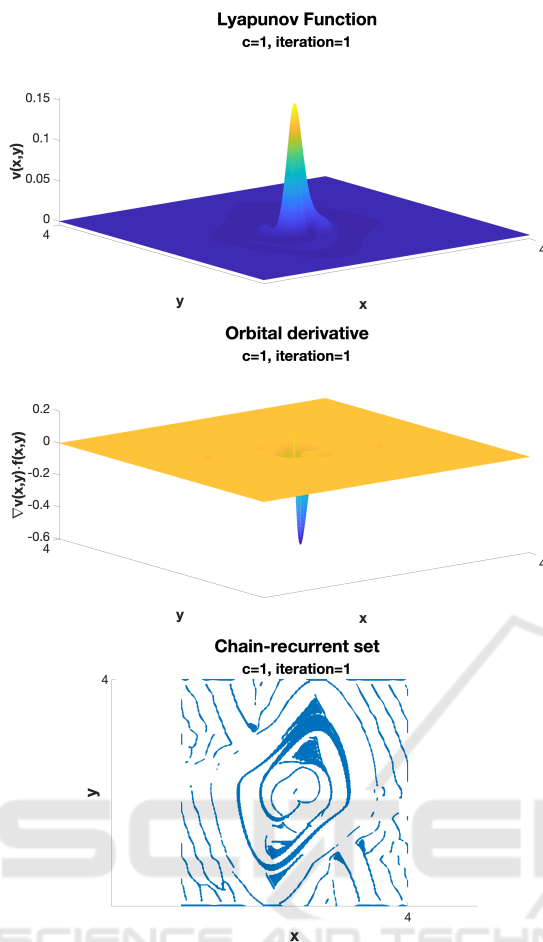


Figure 9: Above: Complete Lyapunov function. Middle: Orbital derivative. Bottom: Chain-recurrent set. System (20). First iteration, i.e., quadratic optimization. The normalized method was used with $c = 1$ and $\delta^2 = 10^{-8}$.

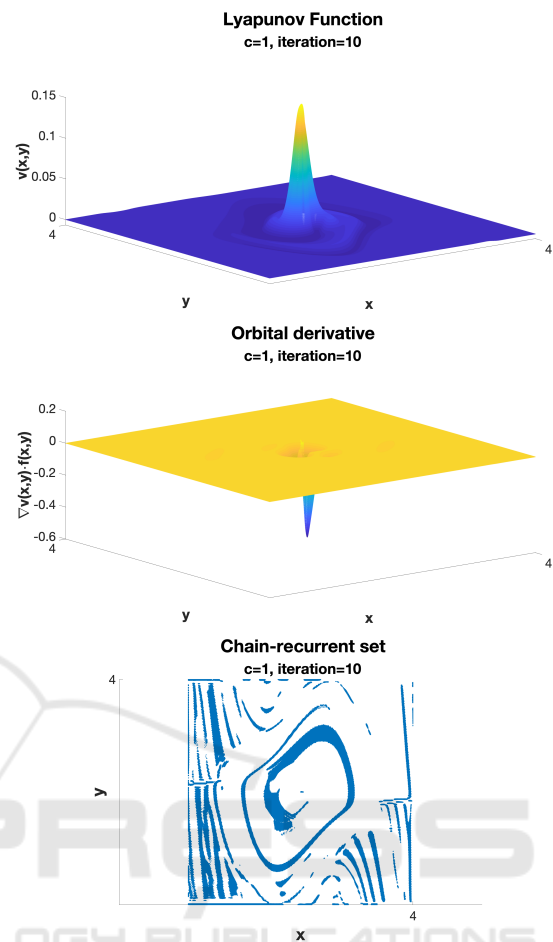


Figure 10: Above: Complete Lyapunov function. Middle: Orbital derivative. Bottom: Chain-recurrent set. System (20). Tenth iteration, i.e., iterative method solving the PDE to the values of the average values of the orbital derivatives around the corresponding collocation points. The normalized method was used with $c = 1$ and $\delta^2 = 10^{-8}$.

Conley, C. (1978). *Isolated Invariant Sets and the Morse Index*. CBMS Regional Conference Series no. 38. American Mathematical Society.

Dellnitz, M., Froyland, G., and Junge, O. (2001). The algorithms behind GAIO – set oriented numerical methods for dynamical systems. In *Ergodic theory, analysis, and efficient simulation of dynamical systems*, pages 145–174, 805–807. Springer, Berlin.

Fathi, A. and Pageault, P. (2019). Smoothing Lyapunov functions. *Trans. Amer. Math. Soc.*, 371:1677–1700.

Giesl, P. (2007). *Construction of Global Lyapunov Functions Using Radial Basis Functions*. Lecture Notes in Math. 1904, Springer.

Giesl, P., Argáez, C., Hafstein, S., and Wendland, H. (2018). Construction of a complete Lyapunov function using quadratic programming. In *Proceedings of the 15th International Conference on Informatics in Control, Automation and Robotics (ICINCO 2018)*, pages 560–568.

Giesl, P. and Wendland, H. (2007). Meshless collocation:

error estimates with application to Dynamical Systems. *SIAM J. Numer. Anal.*, 45(4):1723–1741.

Goullet, A., Harker, S., Mischaikow, K., Kalies, W., and Kasti, D. (2015). Efficient computation of Lyapunov functions for Morse decompositions. *Discrete Contin. Dyn. Syst.*, 20(8):2419–2451.

Hurley, M. (1992). Noncompact chain recurrence and attraction. *Proc. Amer. Math. Soc.*, 115:1139–1148.

Hurley, M. (1998). Lyapunov functions and attractors in arbitrary metric spaces. *Proc. Amer. Math. Soc.*, 126:245–256.

Iske, A. (1998). Perfect centre placement for radial basis function methods. Technical Report TUM-M9809, TU Munich, Germany.

Kalies, W., Mischaikow, K., and VanderVorst, R. (2005). An algorithmic approach to chain recurrence. *Found. Comput. Math.*, 5(4):409–449.

Narcowich, F. J., Ward, J. D., and Wendland, H. (2005). Sobolev bounds on functions with scattered zeros,

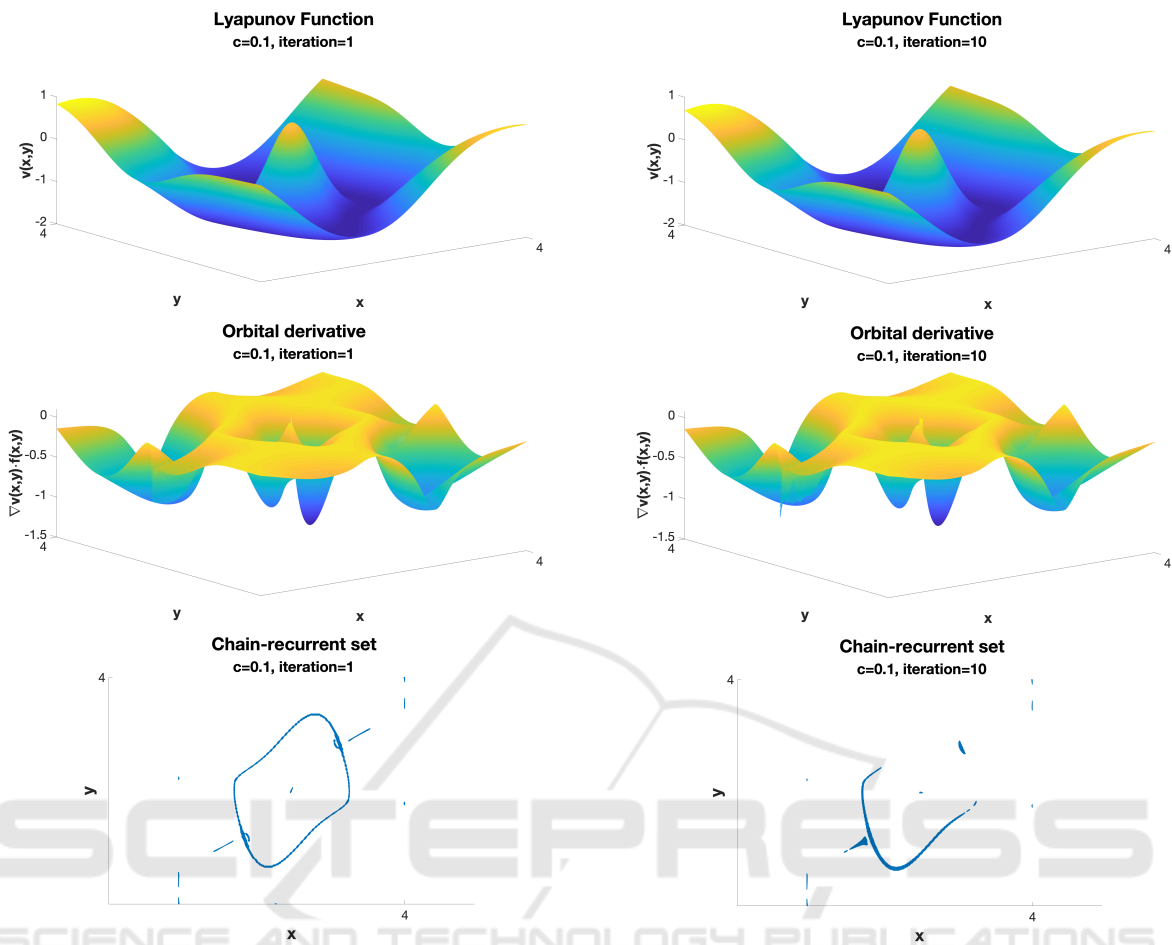


Figure 11: Above: Complete Lyapunov function. Middle: Orbital derivative. Bottom: Chain-recurrent set. System (20). First iteration, i.e., iterative method solving the PDE to the values of the average values of the orbital derivatives around the corresponding collocation points. The normalized method was used with $c = 0.1$ and $\delta^2 = 10^{-8}$.

Figure 12: Above: Complete Lyapunov function. Middle: Orbital derivative. Bottom: Chain-recurrent set. System (20). Tenth iteration, i.e., iterative method solving the PDE to the values of the average values of the orbital derivatives around the corresponding collocation points. The normalized method was used with $c = 0.1$ and $\delta^2 = 10^{-8}$.

with applications to radial basis function surface fitting. *Mathematics of Computation*, 74:743–763.

Suhr, S. and Hafstein, S. (2020). Smooth complete Lyapunov functions for ODEs. *submitted*.

Wendland, H. (1995). Piecewise polynomial, positive definite and compactly supported radial functions of minimal degree. *Adv. Comput. Math.*, 4(4):389–396.

Wendland, H. (1998). Error estimates for interpolation by compactly supported Radial Basis Functions of minimal degree. *J. Approx. Theory*, 93:258–272.

Wendland, H. (2005). *Scattered data approximation*, volume 17 of *Cambridge Monographs on Applied and Computational Mathematics*. Cambridge University Press, Cambridge.